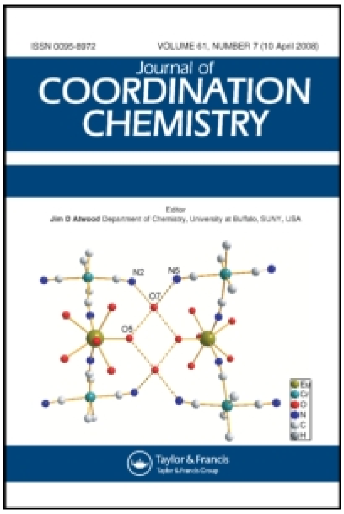

Journal of Coordination Chemistry
Publication details, including instructions for authors and subscription information:
http://www.informaworld.com/smpp/title~content=t713455674

SYNTHESES, CHARACTERIZATION AND CRYSTAL STRUCTURE OF TETRAMETHYLDIBENZOTETRAAZA[14]-ANNULENE ZINC(II) COMPLEXES CONTAINING AN AXIAL BASE

Zenglin Wang[a]; Kazunori Sakata[a]; Mamoru Hashimoto[a]
[a] Department of Chemistry, Faculty of Engineering, Kyushu Institute of Technology, Tobata-ku, Kitakyushu, Japan

To cite this Article Wang, Zenglin , Sakata, Kazunori and Hashimoto, Mamoru(1999) 'SYNTHESES, CHARACTERIZATION AND CRYSTAL STRUCTURE OF TETRAMETHYLDIBENZOTETRAAZA[14]-ANNULENE ZINC(II) COMPLEXES CONTAINING AN AXIAL BASE', Journal of Coordination Chemistry, 48: 4, 541 — 554

To link to this Article: DOI: 10.1080/00958979908023594
URL: http://dx.doi.org/10.1080/00958979908023594

J. Coord. Chem., 1999, Vol. 48, pp. 541–554
Reprints available directly from the publisher
Photocopying permitted by license only

Published by license under
the Gordon and Breach Science
Publishers imprint.
Printed in Malaysia.

SYNTHESES, CHARACTERIZATION AND CRYSTAL STRUCTURE OF TETRAMETHYLDIBENZOTETRAAZA[14]-ANNULENE ZINC(II) COMPLEXES CONTAINING AN AXIAL BASE

ZENGLIN WANG, KAZUNORI SAKATA* and
MAMORU HASHIMOTO

Department of Chemistry, Faculty of Engineering, Kyushu Institute of Technology, Tobata-ku, Kitakyushu 804-8550, Japan

(Received 27 May 1998; Revised 10 December 1998; In final form 10 March 1999)

The complexes of Zn(tmtaa) and Zn(tmtaa)L [H_2tmtaa = tetramethyldibenzotetraaza[14]-annulene; L = triethylamine, pyridine (Py) and *p*-dimethylaminopyridine (*p*-$N(CH_3)_2Py$)] were synthesized and characterized by IR, UV, mass and NMR spectra as well as DSC measurements. The effects of different axial ligands (L) on the spectral properties of the complexes have been studied. The crystal structure of Zn(tmtaa)$N(C_2H_5)_3$ was determined by X-ray diffraction. The crystal belongs to a monoclinic system and the space group is $P2_1/n$. The cell parameters are $a = 11.134(2)$ Å, $b = 17.453(4)$ Å, $c = 13.784(3)$ Å, $\beta = 106.19(3)°$, $Z = 4$, $R_1 = 0.0336$ and $wR_2 = 0.0805$ for 4539 independent reflections with $I > 2\sigma(I)$. The zinc(II) is coordinated through four nitrogen atoms of tmtaa and a nitrogen of triethylamine to form a five-coordinate square-pyramidal structure. The average bond length of Zn for the four nitrogens of tmtaa is 2.050(2) Å and for a nitrogen of triethylamine is 2.188(2) Å. The displacement of the zinc to the plane of four nitrogens of tmtaa is 0.563(2) Å.

Keywords: Zinc(II) complexes; macrocycles; crystal structures; tmtaa complexes; square-pyramidal complexes; NMR spectra

INTRODUCTION

Tetramethyldibenzotetraaza[14]annulene, abbreviated as H_2tmtaa, is a macrocyclic compound of a 14-membered ring and has a structure and

---

* Corresponding author. Fax: (93)884-3300.

properties similar to porphyrins and phthalocyanines. It also features important differences with porphyrins and phthalocyanines such as ring number, core size, extent of conjugation and molecular structure. Thus, similarities to porphyrins make the tmtaa macrocycle of bioinorganic interest, and its peculiarities make it of fundamental interest in its own right.[1–5] Transition-metal tmtaa complexes have been extensively studied.[2b] Syntheses and structures of Fe(II), Fe(III), Co(III), Mn(II) and Mn(III) complexes of H_2tmtaa were reported by Goedken *et al.*[3] Syntheses and structures of Pd(tmtaa) and Co(tmtaa)DME (DME = 1,2-dimethoxyethane) were also studied.[4,5] The synthesis and characterization of Zn(tmtaa)$N(C_2H_5)_3$ were already reported,[6] but the crystal structure of the complex has not been determined. Continuing our research, the complexes of Zn(tmtaa) and Zn(tmtaa)L [L = triethylamine, pyridine (Py) and *p*-dimethylaminopyridine (*p*-$N(CH_3)_2$Py)] were synthesized and characterized. The crystal structure of Zn(tmtaa)$N(C_2H_5)_3$ was determined by X-ray diffraction.

EXPERIMENTAL

Materials and Physical Measurements

All chemicals were reagent grade and were used without further purification except as noted. Solvents were distilled from sodium-benzophenone blue solutions (benzene) or from phosphorus pentoxide (acetonitrile) under a nitrogen atmosphere. Triethylamine was dried over sodium hydroxide and distilled. All reactions were performed under a nitrogen atmosphere. The H_2tmtaa was prepared according to the literature.[7]

Infrared spectra in the 400–4000 cm^{-1} region were obtained on a Hitachi 260-30 spectrophotometer at room temperature with a KBr disk. Ultraviolet and visible spectra covering the 14 000–37 000 cm^{-1} range were recorded on a Shimadzu UV-200S double beam spectrophotometer for benzene solutions at room temperature. ^{1}H-NMR and ^{13}C-NMR spectra were taken on a JEOL JNM-A500 spectrometer operating in a Fourier transform mode. The NMR measurments were run in benzene-d_6 and in chloroform-d. Chemical shifts are given in ppm relative to tetramethylsilane as an internal reference standard. FAB mass spectra in matrices of glycerin were carried out with a JEOL JMS-SX102A gas chromatograph-mass spectrometer. DSC were performed with a Shimadzu Model DT-50 thermal analyzer in a dry nitrogen atmosphere and a heating rate of 10 deg/min. Elemental analyses were determined with a Yanaco CHN Corder MT-3.

Preparation of $Zn(tmtaa)N(C_2H_5)_3$ Complex

The complex $Zn(tmtaa)N(C_2H_5)_3$ was prepared according to the literature.[6] Crystals for X-ray diffraction were obtained by recrystallization from benzene/acetonitrile (2 : 1 vol/vol); yield 52.3% (Ref. [6] yield 56.8%). *Anal.* Calc. for $C_{28}H_{37}N_5Zn$(%): C, 66.07; H, 7.33; N, 13.76. Found: C, 65.98; H, 7.38; N, 13.81. IR (KBr): 1616(m), 1545(s), 1480(s), 1450(s), 1420(s), 1276(m), 1182(s), 1020(m), 745(s).

Preparation of Zn(tmtaa)(*p*-$N(CH_3)_2Py$) Complex

A mixture of H_2tmtaa (0.688 g, 2.0 mmol), *p*-$N(CH_3)_2Py$ (0.976 g, 8.0 mmol), $Zn(SO_3CF_3)_2$ (0.728 g, 2.0 mmol) and methanol (40 mL) was refluxed under a nitrogen atmosphere for 1.5 h. After the reaction mixture cooled to room temperature, the precipitate was recovered by filtration and washed with methanol to give a dark red powder. The complex was recrystallized from benzene/acetonitrile (1 : 1 vol/vol), and dark red crystals were obtained; yield 0.514 g (48.2%). *Anal.* Calc. for $C_{29}H_{32}N_6Zn$(%): C, 65.72; H, 6.09; N, 15.86. Found: C, 65.73; H, 6.26; N, 16.01. IR (KBr): 1616(m), 1541(s), 1466(s), 1450(s), 1418(s), 1276(m), 1228(m), 1186(s), 1022(m), 1010(m), 804(m), 745(s).

Preparation of Zn(tmtaa) Complex

Ground powder of $Zn(tmtaa)N(C_2H_5)_3$ was put into a vacuum oven at 80°C and 1 mmHg for 12 h. The triethylamine was lost, and Zn(tmtaa) was obtained. *Anal.* Calc. for $C_{22}H_{22}N_4Zn$(%): C, 64.79; H, 5.44; N, 13.74. Found: C, 64.19; H, 5.50; N, 13.69. IR (KBr): 1616(m), 1540(s), 1470(s), 1455(s), 1280(m), 1190(s), 1028(m), 745(s).

Preparation of Zn(tmtaa)Py and Zn(tmtaa)Py · $2C_6H_6$ Complexes

A mixture of Zn(tmtaa) (0.407 g, 1.0 mmol), Py (0.316 g, 4.0 mmol) and acetonitrile (15 mL) was refluxed under a nitrogen atmosphere with stirring for 12 h. After the reaction mixture cooled to room temperature, the red powder was collected by filtration and washed with acetonitrile. When the product was recrystallized from acetonitrile, Zn(tmtaa)Py was obtained; in benzene, Zn(tmtaa)Py · $2C_6H_6$ was obtained. For Zn(tmtaa)Py, the yield was 0.409 g (77.2%). *Anal.* Calc. for $C_{27}H_{27}N_5Zn$(%): C, 66.60; H, 5.59; N, 14.38. Found: C, 66.52; H, 5.77; N, 14.43. IR (KBr): 1616(m), 1547(s), 1450(s), 1416(s), 1272(m), 1182(s), 1020(m), 740(s). For Zn(tmtaa)Py · $2C_6H_6$, the yield was 0.443 g (69.0%). *Anal.* Calc. for $C_{39}H_{39}N_5Zn$(%): C, 72.83; H, 6.11; N, 10.89. Found: C, 72.07; H, 6.21; N, 11.30. IR (KBr): 1616(s), 1566(s), 1470(s), 1450(s), 1416(s), 1380(m), 1360(m), 1344(m), 1320(m), 1184(s), 1022(m), 1010(m), 800(m), 740(s).

X-ray Crystallography

Red crystals of Zn(tmtaa)N(C_2H_5)$_3$ were selected and mounted on glass fibers. X-ray data were collected on a Siemens P4 four circle diffractometer by means of an ω-scan and MoK_α radiation at room temperature. The cell parameters and an orientation matrix for data collection were obtained from the least squares refinement of the diffraction data from 25 reflections. The three check reflections measured with 100 reflections show no decay in intensity. The data were corrected by Lorentz-polarization factors and the empirical absorption correction. The structure was solved by standard heavy atom methods and refined by full-matrix least-squares methods. All non-hydrogen atoms of the complex were refined anisotropically. All hydrogen atoms of the complex were located on a difference Fourier map. A summary of the crystal data, the experimental detail and the refined results are listed in Table I.

TABLE I Crystallographic data for Zn(tmtaa)N(C_2H_5)$_3$

Empirical formula	$C_{28}H_{37}N_5Zn$
Formula weight	509.00
Temperature	293(2) K
Wavelength	0.71073 Å
Crystal system	Monoclinic
Space group	$P2_1/n$
Unit cell dimensions	$a = 11.134(2)$ Å, $\alpha = 90°$ $b = 17.453(4)$ Å, $\beta = 106.19(3)°$ $c = 13.784(3)$ Å, $\gamma = 90°$
Volume, Z	2572.3(9) Å^3, 4
Density (calculated)	1.314 Mg/m^3
Absorption coefficient	0.980 mm^{-1}
$F(000)$	1080
Crystal size	0.48 × 0.42 × 0.40 mm
θ Range for data collection	1.93–25.01°
Limiting indices	$-1 \le h \le 13$, $-1 \le k \le 20$, $-16 \le l \le 16$
Reflections collected	5855
Independent reflections	4539 ($R_{int} = 0.0248$)
Max. and Min. transmission	0.60268 and 0.57273
Refinement method	Full-matrix least-squares on F^2
Data/restraints/parameters	4539/0/455
Goodness-of-fit on F^2	0.705
Final R indices [$I > 2\sigma$]	$R_1 = 0.0336$, w$R_2 = 0.0805$
Largest diff. peak and hole	0.203 and −0.276 e Å^{-3}

$R_1 = \sum||F_o| - |F_c||/\sum|F_o|$. $wR_2 = \{\sum[w(F_o^2 - F_c^2)^2]/\sum[w(F_o^2)^2]\}^{1/2}$.
GOOF $= s = \{\sum[w(F_o^2 - F_c^2])^2]/(n-p)\}^{1/2}$.

RESULTS AND DISCUSSION

Syntheses and Characterization of Zn(tmtaa) and Zn(tmtaa)L Complexes

Zn(tmtaa)N$(C_2H_5)_3$ could be prepared according to the literature,[6] but Zn(tmtaa)(*p*-N$(CH_3)_2$Py) could not be obtained by the same method. The latter complex was synthesized by refluxing a mixture of H_2tmtaa, Zn$(SO_3CF_3)_2$ and *p*-N$(CH_3)_2$Py for 1.5 h with stirring. For Zn(tmtaa)Py, it is difficult to prepare the complex by direct reaction of H_2tmtaa with Zn$(SO_3CF_3)_2$ in excess pyridine because of the weaker basicity of pyridine.

The complexes were characterized by IR, UV, mass and NMR spectra as well as DSC measurements. UV, mass spectra and DSC data are compiled in Table II. The IR spectra of Zn(tmtaa)L are similar to those of Zn(tmtaa) except for bands of the axial ligands and are different from those of H_2tmtaa. The IR bands of H_2tmtaa at 1620(s), 1600(m), 1554(s) and 1512(s) are assigned C=N and C=C stretching modes.[8] After formation of the complexes, the IR bands shift to lower frequency at 1540(s), 1470(s) and 1455(s). Comparing Zn(tmtaa) with Zn(tmtaa)L, the band positions for C=N and C=C stretching modes are slightly different.

The electronic absorption spectra for the complexes were measured in benzene solution at room temperature. The electronic spectra of all zinc complexes are similar with two absorption bands at about 380 and 410 nm (shoulder). Comparing a maximum absorption band (348 nm) of H_2tmtaa with that of Zn(tmtaa) shows a 33.5 nm shift to longer wavelength, which may be attributed to $\pi \rightarrow \pi^*$ transitions within a ligand molecule and CT transitions from metal to ligand.[9] When an axial ligand is coordinated to the zinc ion and the five-coordinate complexes formed, the maximum bands (about 380 nm) of the complexes were shifted to a shorter wavelength by only 3–5.5 nm. This seems to indicate that coordination of the axial ligands causes displacement of the zinc ion from the plane of nitrogens. The complexes are stable as solids, but are not stable in solution for Zn(tmtaa) and Zn(tmtaa)N$(C_2H_5)_3$. Though the basicity of N$(C_2H_5)_3$ is the strongest of the axial ligands, the order of stability within the complexes is Zn(tmtaa)(*p*-N$(CH_3)_2$Py) > Zn(tmtaa)Py > Zn(tmtaa)N$(C_2H_5)_3$ > Zn(tmtaa). This presumably explains that the stability of the complexes is balanced for the basicity and π-back donation of the axial ligands.

The FAB mass spectra establish the presence of molecular ions $[M+1]^+$ at *m/z* 407, 508 and 529, for Zn(tmtaa), Zn(tmtaa)N$(C_2H_5)_3$ and Zn(tmtaa)(*p*-N$(CH_3)_2$Py), respectively. On the other hand, Zn(tmtaa)Py shows a cluster of ions corresponding to $[M+1-\text{Py}]^+$ at *m/z* 407. For all

TABLE II Physical and chemical properties of zinc complexes

Complex	*Electronic absorption spectra*				*Data of DSC**		*Mass spectral data*		
	λ_{max} (nm)	$\log\varepsilon$	λ_{max} (nm)	$\log\varepsilon$	T_1 (°C)	T_2 (°C)	*Calcd.*	*Obsd.*	*Base peak*
H_2tmtaa	348.0	4.63				243.4	344	344 M^+	344 M^+
Zn(tmtaa)	381.5		411			392.3	406	407 $[M+1]^+$	407 $[M+1]^+$
Zn(tmtaa)$N(C_2H_5)_3$	378.5		410		161.1	392.0	507	508 $[M+1]^+$	407 $[M+1-N(C_2H_5)_3]^+$
Zn(tmtaa)Py	376.5	4.83	410	4.17	239.4	392.7	485	407 $[M+1-Py]^+$	407 $[M+1-Py]^+$
Zn(tmtaa)Py · $2C_6H_6$	376.5	4.83	410	4.17	91.6, 229.4	393.0			
Zn(tmtaa)(p-$N(CH_3)_2$Py)	377.0	5.01	410	4.40	312.3	391.8	528	529 $[M+1]^+$	407 $[M+1]-(p\text{-}N(CH_3)_2Py)]^+$

*T_1: temperature of lost crystalline solvents and lost axial ligands; T_2: temperature of a melting point.

complexes, the base peaks of the mass spectra are at m/z 407, which corresponds to $[\mathrm{Zn(tmtaa)} + 1]^+$.

The DSC data show that thermal decomposition of the complexes is divided into three kinds. Zn(tmtaa) only reveals a melting process at 392.8°C, and then decomposes. Zn(tmtaa)$N(C_2H_5)_3$, Zn(tmtaa)Py and Zn(tmtaa)(p-$N(CH_3)_2$Py) first lose the axial ligands and subsequently produce Zn(tmtaa), which passes the smelting process and decomposes. On the other hand, Zn(tmtaa)Py · $2C_6H_6$ loses the benzene at first, and then gives the same process as Zn(tmtaa)Py.

The zinc(II) complexes gave well-resolved proton NMR spectra. The chemical shift assignments were accomplished on the basis of comparison with H_2tmtaa and are compiled in Table III. The proton signal of the amine disappears on formation of the complexes. The methyl proton signal of Zn(tmtaa) is shifted downfield and the methine proton signal is shifted upfield in comparison with H_2tmtaa. The downfield shift and upfield shift of the proton signals in the complexes are associated with the change of electron density of the protons. When the non-conjugate 2,4-pentanediminato rings of H_2tmtaa became delocalized after complex formation (see the crystal structure results), the distribution of electron density in the ligand varied. Since the distances of the methyl group and/or of the methine group from the positive zinc ion are different, the inductive effect from the zinc(II) is different. This variation of electron density is confirmed by carbon-13 NMR for the complexes. When the axial ligand is coordinated to Zn(tmtaa), the methyl, methine and aromatic proton signals are shifted downfield. The amount of shift for the proton signals is different for different axial ligands. Though the basicity of $N(C_2H_5)_3$ is largest at the axial ligands, the methine proton signal of Zn(tmtaa)$N(C_2H_5)_3$ is shifted downfield only 0.119 ppm in comparison with Zn(tmtaa). However, the methine proton signals of Zn(tmtaa)Py and Zn(tmtaa)(p-$N(CH_3)_2$Py) are shifted downfield by 0.231 and 0.251 ppm, respectively. This larger downfield shift is due to ring current effects of the pyridine ring in Py and (p-$N(CH_3)_2$Py).[10]

The proton NMR signals of the axial ligands are well-resolved (see Table III and Scheme 1).

^{13}CNMR data and their assignments for the zinc complexes are collected in Table IV. All methyl peaks in the zinc complexes show downfield shifts of 2.5–3.1 ppm in comparison with H_2tmtaa, while the carbon peaks at the 8- and 17-positions bonded to the olefinic methine exhibit slight upfield shifts. These are in agreement with the results of the proton NMR except for Zn(tmtaa)Py and Zn(tmtaa)(p-$N(CH_3)_2$Py) which have ring current effects. The aromatic carbon peaks at 2-, 5-, 11-, 14-, 3-, 4- 12- and 13-positions

TABLE III ^{1}H-NMR data for H_2tmtaa and zinc complexes[a]

Complex	*Macrocyclic skeleton*				*Others*		
	Methyl	*Methine*	*Aromatic*				
H_2tmtaa	1.878(s)	4.694(s)	6.897(m),	6.870(m)	13.10(s) (N–H)		
Zn(tmtaa)	2.101(s)	4.558(s)	6.898(m),	6.875(m)			
Zn(tmtaa)N(C_2H_5)$_3$	2.112(s)	4.677(s)	6.980(m),	6.910(m)	0.838(t) (–CH_3), $J = 7.14$ Hz	2.521(q) (–CH_2–) $J = 7.14$ Hz	
Zn(tmtaa)Py	2.190(s)	4.794(s)	7.035(m),	6.991(m)	8.143(d) (H_α), $J = 6.56$ Hz	6.229(t) (H_β), $J = 6.56$ Hz	6.493(t) (H_γ) $J = 6.56$ Hz
Zn(tmtaa)(*p*-N(CH_3)$_2$Py)	2.226(s)	4.809(s)	7.116(m),	6.925(m)	7.804(d) (H_α), $J = 6.10$ Hz	5.446(d) (H_β), $J = 6.10$ Hz	3.077(s) (–N(CH_3)$_2$)

[a] *Chemical shifts are given in ppm for TMS. Measured in benzene-d_6.* Multiplicity of a proton singal is given parentheses after δ-value: s = singlet, d = doublet, t = triplet, q = quartet, m = multiplet.

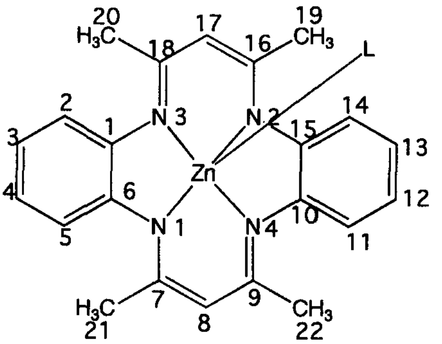

Zn(tmtaa)L $(L = N(C_2H_5)_3$; Py; $p\text{-}N(CH_3)_2Py)$

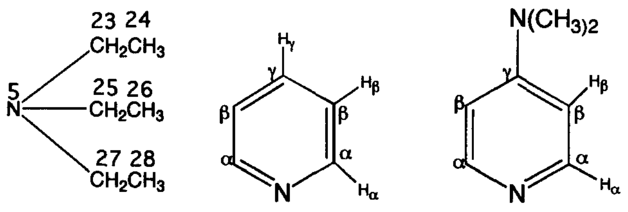

$N(C_2H_5)_3$ Py $p\text{-}N(CH_3)_2Py$

SCHEME 1

show slight upfield shifts in comparison with H_2tmtaa. On the other hand, the aromatic carbon peaks at 1-, 6-, 10- and 15-positions bonded to the nitrogen atoms exhibit apparent downfield shifts. The signals of the olefinic carbons at 7-, 9-, 16- and 18-positions are observed at lower field (1.6–3.9 ppm) than those of H_2tmtaa. The carbon peaks of the axial ligands are compatible with the proton NMR spectra.

Crystal Structure of Zn(tmtaa)$N(C_2H_5)_3$ Complex

An ORTEP of Zn(tmtaa)$N(C_2H_5)_3$ is shown in Figure 1 and the selected bond lengths and selected bond angles are listed in Table V. The structure reveals that the zinc(II) ion is coordinated though four nitrogen atoms of tmtaa and one nitrogen atom of triethylamine to form a five-coordinate complex of square-pyramidal geometry. The macrocyclic ligand has a markedly nonplanar, saddle shape similar to Mn(tmtaa)$N(C_2H_5)_3$.[3(d)] The bond lengths of Zn for the four nitrogen atoms of tmtaa are almost

TABLE IV ^{13}C NMR data for H_2tmtaa and zinc complexes[a]

Complex	$-CH_3$	C_8 C_{17}	C_2 C_5 C_{11} C_{14}	C_3 C_4 C_{12} C_{13}	C_1 C_6 C_{10} C_{15}	C_7 C_9 C_{16} C_{18}	C_α	C_β	C_γ	p-$N(CH_3)_2$	$N{-}CH_2{-}$	$H_3C{-}(CH_2N)$
H_2tmtaa[b]	20.8	98.7	122.5	122.7	138.1	158.4						
Zn(tmtaa)	23.9	97.4	121.6	121.9	140.9	162.3						
Zn(tmtaa)$N(C_2H_5)_3$	23.6	96.7	121.4	122.3	142.8	160.1					45.8	9.6
Zn(tmtaa)Py	23.4	97.2	121.4	122.5	142.8	160.4	148.4	124.4	137.7			
Zn(tmtaa)(p-$N(CH_3)_2$Py)	23.3	96.8	121.2	122.5	143.3	160.0	154.6	106.4	147.8	38.9		

[a] Chemical shifts are given in ppm for TMS. Measured in chloroform-d at room temperature. [b] Ref. [11].

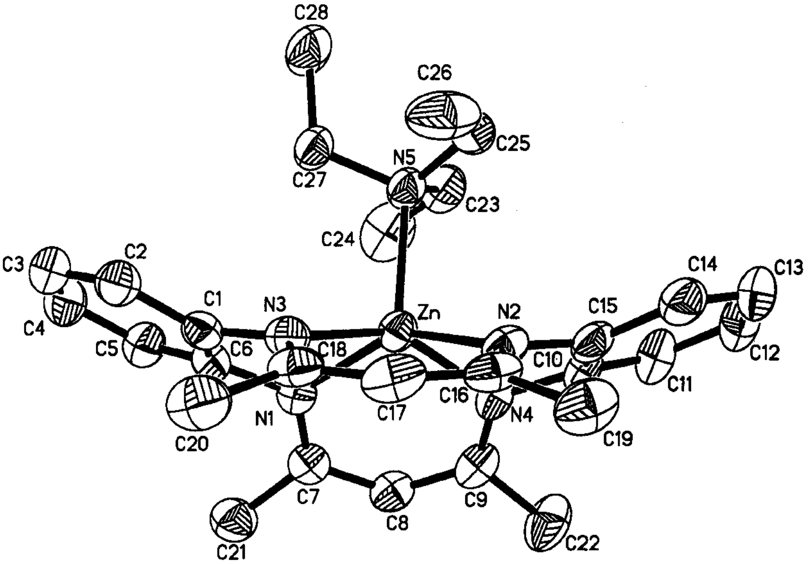

FIGURE 1 ORTEP of Zn(tmtaa)N(C_2H_5)$_3$.

TABLE V Selected bond lengths [Å] and selected bond angles [°]

Zn–N(2)	2.034(2)	Zn–N(3)	2.053(2)
Zn–N(1)	2.054(2)	Zn–N(4)	2.057(2)
Zn–N(5)	2.188(2)	N(1)–C(7)	1.321(3)
N(1)–C(6)	1.403(3)	N(2)–C(16)	1.328(4)
N(2)–C(15)	1.403(4)	N(3)–C(18)	1.327(3)
N(3)–C(1)	1.402(4)	N(4)–C(9)	1.323(4)
N(4)–C(10)	1.404(4)	N(5)–C(27)	1.488(4)
N(5)–C(23)	1.491(4)	N(5)–C(25)	1.494(4)
C(7)–C(8)	1.407(4)	C(8)–C(9)	1.394(4)
C(16)–C(17)	1.398(4)	C(17)–C(18)	1.403(4)
N(2)–Zn–N(3)	92.60(9)	N(2)–Zn–N(1)	146.76(9)
N(3)–Zn–N(1)	79.33(9)	N(2)–Zn–N(4)	79.57(9)
N(3)–Zn–N(4)	149.44(9)	N(1)–Zn–N(4)	91.12(9)
N(2)–Zn–N(5)	105.24(9)	N(3)–Zn–N(5)	104.78(9)
N(1)–Zn–N(5)	108.00(9)	N(4)–Zn–N(5)	105.77(9)
C(7)–N(1)–C(6)	124.9(2)	C(7)–N(1)–Zn	124.8(2)
C(6)–N(1)–Zn	108.1(2)	C(16)–N(2)–C(15)	126.7(2)
C(16)–N(2)–Zn	124.6(2)	C(15)–N(2)–Zn	108.2(2)
C(18)–N(3)–C(1)	126.0(2)	C(18)–N(3)–Zn	123.9(2)
C(1)–N(3)–Zn	108.3(2)	C(9)–N(4)–C(10)	125.9(2)
C(9)–N(4)–Zn	124.1(2)	C(10)–N(4)–Zn	107.6(2)
C(27)–N(5)–C(23)	111.3(2)	C(27)–N(5)–C(25)	110.4(2)
C(23)–N(5)–C(25)	107.8(3)	C(27)–N(5)–Zn	109.2(2)
C(23)–N(5)–Zn	109.4(2)	C(25)–N(5)–Zn	108.7(2)

equivalent and the average bond length is 2.050(2) Å, which is longer than that of Mn(tmtaa)(NCS) (1.958(2) Å), and Fe(tmtaa)Cl (2.002(2) Å), but is shorter than that of Mn(tmtaa)N(C_2H_5)$_3$ (2.118(3) Å).[3(d)] Though the distance of the metal-donor atoms is correlated with the number of atoms in macrocylic rings and the extent of the ligand conjugation, the coordination number of metal ions is also important to the distance of the metal-donor atoms. For four-coordinate Fe(tmtaa) and five-coordinate Fe(tmtaa)Cl, the Fe–N bond lengths are 1.918(3) and 2.002(2) Å, respectively.[3(c),(d)] This may be attributed to the displacement of the iron from the equatorial plane and the steric hindrance between the macrocyclic ligand and the axial ligand. Consequently, the metal-donor distance for a higher coordination-number complex is not only lengthened in the equatorial bond length, but also the bond length from the metal to the axial ligand is lengthened. The bond length of Zn for the nitrogen atom of triethylamine is 2.188(2) Å in Zn(tmtaa)N(C_2H_5)$_3$. The M–N distance for the five-coordinate complexes of H_2tmtaa and the empirical crystal ionic radii of metal atoms are summarized in Table VI. The data in Table VI show that the distance of M–N in the complexes is lengthened with increasing the metal ion size.

After formation of the complex, the four C–N bond lengths in two six-membered rings are approximately equivalent and the average bond length is 1.325(4) Å which shows more double bond character. The four C–C bond lengths in two six-membered rings are also equivalent and the average bond length is 1.400(4) Å which is longer than that of a C=C double bond and is shorter than that of a C–C single bond.[3(c)] The average C–N distance in the five-membered chelate ring shows more single bond character.

The four nitrogen atoms of tmtaa are coplanar and the average atomic deviation from the plane is 0.022(3) Å. When Zn(tmtaa) is coordinated to an axial ligand, the displacement of Zn from the nitrogen atom plane is increased. This seems to indicate that the steric hindrance between the

TABLE VI Average M–N distance for five-coordinate complexes of H_2tmtaa and empirical crystal ionic radii of metal atoms

Complex	*M–N* (Å)	*Ionic radii* (Å)[a]	*Reference*
Zn(tmtaa)N(C_2H_5)$_3$	2.050(2)	0.82	This paper
[Mn(tmtaa)(NCS)]$_2$ · CH_3CN	1.958(7)	0.72	12
Fe(tmtaa)Cl	2.002(2)	0.72	3
Co(tmtaa)I	1.901(3)	0.685	3
Mn(tmtaa)N(C_2H_5)$_3$	2.118(3)	0.81	3
Mn(tmtaa)(NCS)	1.958(2)	0.72	4
Cr(tmtaa)Cl · C_6H_6 · 1/2C_6H_{12}	1.971(6)	0.775	14

[a] See Ref. [13].

macrocyclic ligand and the axial ligand may prevent the metal ion from sitting in the plane. Hence, the displacement of Zn from the 4N atom plane of tmtaa is 0.563(3) Å, larger than that of Mn(tmtaa)(NCS) (0.356 Å)[3(a)] and smaller than that of Mn(tmtaa)N$(C_2H_5)_3$ (0.730 Å) and Fe(tmtaa)Cl (0.600 Å).[3(c)]

Supplementary Material

The bond lengths and bond angles, hydrogen atom positions, anisotropic thermal parameters of the non-hydrogen atoms, stereoview of the unit cell packing, selected torsion angles and least-squares planes are all available from the authors on request.

Acknowledgments

We thank the Changchun Institute of Applied Chemistry of P.R. China for X-ray structure determination. We are grateful to the Center for Instrumental Analysis, Kyushu Institute of Technology for elemental analyses, mass spectra and NMR spectra.

References

[1] (a) M.L. Chen and A. Tulinsky, *J. Am. Chem. Soc.*, **94**, 4144 (1972); (b) P.W. Codding and A. Tulinsky, *J. Am. Chem. Soc.*, **94**, 4151 (1972).
[2] (a) V.L. Goedken, J.J. Pluth, S.M. Peng and B. Bursten, *J. Am. Chem. Soc.*, **98**, 8014 (1976); (b) F.A. Cotton and J. Czuchajowska, *Polyhedron*, **9**, 2553 (1990).
[3] (a) V.L. Goedken, S.M. Peng and Y. Park, *J. Am. Chem. Soc.*, **76**, 284 (1974); (b) M.C. Weiss and V.L. Goedken, *Inorg. Chem.*, **18**, 274 (1979); (c) V.L. Goedken, J.J. Pluth, S.M. Peng and B. Bursten, *J. Am. Chem. Soc.*, **98**, 8014 (1976); (d) M.C. Weiss, B. Bursten, S.M. Peng and V.L. Goedken, *J. Am. Chem., Soc.*, **98**, 8021 (1976).
[4] M. Tsutsui, R.L. Bobsein, G. Cash and R. Pettersen, *Inorg. Chem.*, **18**, 758 (1979).
[5] J. Magull and A. Simon, *Z. Anorg. Allg. Chem.*, **615**, 81 (1992).
[6] D.R. Neves and J.C. Dabrowiak, *Inorg. Chem.*, **15**, 129 (1976).
[7] (a) V.L. Goedken and J. Molin-Case, *J. Chem. Soc., Chem. Commun.*, 337 (1992); (b) K. Sakata, F. Yamaura and M. Hashimato, *Synth. React. Inorg. Met.-Org. Chem.*, **20**, 1043 (1990).
[8] (a) D.J. Olszanski and G.A. Melson, *Inorg. Chim. Acta*, **23**, L4 (1977); (b) G.R. Willey and M.D. Rudd, *Polyhedron*, **11**, 2805 (1992); (c) K. Sakata, M. Hashimoto, T. Hamada and S. Matsuno, *Polyhedron*, **15**, 967 (1996).
[9] (a) K. Sakata and T. Hori, *Synth. React. Inorg. Met.-Org. Chem.*, **20**, 263 (1990); (b) K. Sakata and A. Ueno, *Synth. React. Inorg. Met.-Org. Chem.*, **21**, 729 (1991); (c) K. Sakata and M. Itoh, *J. Heterocyclic Chem.*, **29**, 921 (1992); (d) K. Sakata, A. Ueno, T. Jibuta and M. Hashimoto, *Synth. React. Inorg. Met.-Org. Chem.*, **23**, 1107 (1993); (e) K. Sakata, K. Koyanagi and M. Hashimoto, *J. Heterocyclic Chem.*, **32**, 329 (1995); (f) K. Sakata, M. Shimoda and M. Hashimoto, *J. Heterocyclic Chem.*, **33**, 1593 (1996).

[10] M.R. Silverstein and G.C. Bassler, *Spectrometric Identification of Organic Compounds* (John Wiley & Sons Inc., New York, 1963), p. 116.

[11] K. Sakata, H. Tagami and M. Hashimoto, *J. Hetrocyclic Chem.*, **26**, 805 (1989).

[12] K. Sakata, Z. Wang and M. Hashimoto, *Synth. React. Inorg. Met.-Org. Chem.*, **29**, 265 (1999).

[13] R.D. Shannon, *Acta Crystallogr.*, **A 32**, 751 (1976).

[14] F.A. Cotton, J. Czuchajowska, L.R. Falvello and X. Feng, *Inorg. Chim. Acta*, **172,** 135 (1990).